

## Flow Stability Investigation in Parallel Channels with Supercritical Water by Comparing Axially Decreased and Homogeneous Axial Power Shapes: A Review

Edward Shitsi, Seth Kofi Debrah, Vincent Yao Agbodemegbe, Emmanuel Ampomah-Amoako and Henry Cecil Odoi

*Department of Nuclear Engineering, School of Nuclear and Allied Sciences, University of Ghana, P.O. Box AE 1, Atomic Energy, Kwabenya, Accra, Ghana*

**Key words:** Dimensional and dimensionless parameters, supercritical pressure, flow instability, axial power distributions, stability boundary, parallel channel

**Abstract:** Research into flow instability has attracted attention of many scientists and engineers in recent years because of its importance in water-cooled and water moderated nuclear reactors and steam generators at both subcritical and supercritical pressures. Supercritical Water-cooled Reactor SCWR, a GEN IV reactor is prone to flow instability just like Boiling Water Reactor BWR because of drastic variations in fluid properties at the vicinity of the pseudo-critical temperature. Flow instability at supercritical pressures needs to be addressed as it is undesirable and can threaten design safety limits and eventually cause mechanical damage of heat transfer equipment. This study seeks to examine two flow instability analysis methods used to describe flow instability results. The flow instability analysis methods including dimensional and dimensionless stability diagrams (dimensional and Ambrosini's dimensionless parameters) were adopted to obtain stability boundaries for the various systems considered in this work. Axially decreased and homogeneous axial power shapes/distributions were adopted in heating the heated channels/sections of the parallel channel system considered. This study examines also the influences of parameters including mass flow rate, pressure and gravity on flow instability at supercritical pressures in parallel channels. Data used for the study were obtained from literature. The results show that both the dimensional and dimensionless stability diagrams could be used for flow instability analysis as the two different types of stability diagrams almost produced the same findings in this research. The following additional findings were obtained during the investigation using both the dimensional and dimensionless stability diagrams. At low mass flow rates, stability of the system with HAPS (Homogeneous Axial Power Shape) or ADPS (Axially Decreased Power Shape)

### Corresponding Author:

Edward Shitsi

*Department of Nuclear Engineering, School of Nuclear and Allied Sciences, University of Ghana, P.O. Box AE 1, Atomic Energy, Kwabenya, Accra, Ghana*

Page No.: 2998-3009

Volume: 15, Issue 15, 2020

ISSN: 1816-949x

Journal of Engineering and Applied Sciences

Copy Right: Medwell Publications

decreases and increases respectively below and above a certain threshold power with inlet temperature. At high mass flow rates, there is a threshold power below which stability decreases and above which stability increases with inlet temperature for HAPS but there is only lower threshold for ADPS and the stability decreases with inlet temperature. The system with HAPS is more stable than that with ADPS. The type of axial power shape adopted in supplying heat to the fluid flowing through heat transfer system has significant effect on the stability of the system. Comparing the numerical results with

experimental results, the 3D numerical tool, STAR-CCM+CFD code could predict flow instability in the parallel channels irrespective of the type of axial power shape adopted. The numerical tool could predict experimental results quite better for a system with HAPS than that with ADPS. The numerical tool adopted largely under-predicted experimental amplitude and quite well predicted experimental period of the inlet mass flow oscillations. Supercritical systems operated under 25 MPa are more stable than those operated under 23 MPa.

## INTRODUCTION

Research into flow instability has attracted attention of many scientists and engineers in recent years because of its importance in water-cooled and water moderated nuclear reactors and steam generators at both subcritical and supercritical pressures. SCWR, a GEN IV reactor is prone to flow instability just like BWR because of drastic variations in fluid properties at the vicinity of the pseudo-critical temperature<sup>[1-3]</sup>. Flow instability at supercritical pressures need to be addressed as it is undesirable and can threaten design safety limits and eventually cause mechanical damage of heat transfer equipment. The designer of such heat transfer related equipment must be able to predict the threshold of flow instability in order to design around it or compensate for it<sup>[4-7]</sup>.

Generally, three similar dimensionless parameters based on 1D Model that are used to describe flow instability boundary are provided by Gomez *et al.*<sup>[8]</sup> Ambrosini and Sharabi<sup>[9]</sup>. There are several investigations in recent years that are devoted to addressing flow instability at supercritical pressures adopting these 1D dimensionless parameters to develop flow instability boundaries. These investigations include numerical researches by Ambrosini and Sharabi<sup>[10]</sup>, Ambrosini<sup>[11]</sup>, Ambrosini and Sharabi<sup>[9]</sup>, Sharabi<sup>[12]</sup>, Gomez *et al.*<sup>[18]</sup>, Gomez<sup>[13]</sup>, Ambrosini<sup>[14]</sup>, Ampomah-Amoako and Ambrosini<sup>[15]</sup>, Ampomah-Amoako<sup>[6]</sup>, Debrah *et al.*<sup>[16, 17]</sup>, Xiong *et al.*<sup>[18]</sup>, Li *et al.*<sup>[19]</sup> and experimental researches by Xiong *et al.*<sup>[20]</sup> and Zhang *et al.*<sup>[21]</sup> among others. There are other studies addressing flow instability adopting dimensional parameters to develop flow instability boundaries. These studies include some numerical researches by Xi *et al.*<sup>[22]</sup>, Hou *et al.*<sup>[23]</sup>, Su *et al.*<sup>[24]</sup> and Xiong *et al.*<sup>[18]</sup> and experimental researches by Xiong *et al.*<sup>[20]</sup> and Xi *et al.*<sup>[22]</sup>.

Xi *et al.*<sup>[22]</sup> made use of three Dimensional (3D) CFX code and performed flow instability analysis investigating an out of phase oscillation in parallel channels with water at supercritical pressure. Standard k- $\epsilon$  turbulence model

was selected for 3D numerical simulations based on the sensitivity analysis performed on some selected turbulence models. Results show that the 3D code could predict the onset of flow instability better than 1D code but could not predict the period of oscillation, i.e., the 3D numerical estimation of the oscillation period is much longer than that of the experiment. The results by Xi *et al.*<sup>[3, 22]</sup> also show that instability of a system is influenced by mass flow rate, pressure and gravity based on the obtained instability boundaries. That is the system is less stable to operate at high mass flow rate and at high pressure. The system is more stable when operated without the influence of gravity. Shitsi *et al.*<sup>[25]</sup> investigated flow instability in two parallel channels with supercritical water under different system pressures, inlet mass flow rates, inlet temperatures and axial power shapes using STAR-CCM+ CFD code. Standard k- $\epsilon$  turbulence model was selected for 3D numerical simulations based on the sensitivity analysis performed on some selected turbulence models. They found out that the system parameters have significant effect on the amplitude of the mass flow oscillation and maximum temperature of the heated outlet temperature oscillation but have little effect on the period of the mass flow oscillation. A system with larger amplitude of flow oscillation is more unstable. Sharabi<sup>[12]</sup> also carried out flow instability analysis on circular pipe at supercritical pressure adopting k- $\epsilon$  turbulence model implemented in FLUENT CFD code. It was observed that heat transfer deterioration could occur before the occurrence of unstable behavior at supercritical conditions. Li *et al.*<sup>[19]</sup> carried out 3-D simulation of water at supercritical pressure in parallel channels in order to investigate flow instability. SST turbulence model was selected for 3D numerical simulations. It was observed that system stability increases with inlet mass flow rate and the effect of inlet temperature on flow instability is not linear. Li *et al.*<sup>[19]</sup> observed also that there is particular threshold inlet temperature below which stability decreases and above which stability increases with inlet temperature. Ebrahimnia *et al.*<sup>[26]</sup> adopted CFD code ANSYS CFX

v14.5 to analyze static and oscillatory flow instabilities in a vertical pipe of SCW flowing upward using the  $k-\epsilon$  turbulence model with a scalable wall-function and the  $k-\omega$ -based SST turbulence model. The marginal stability boundary results of the CFD code were compared with the predictions of 1-D non-linear code. They observed that there was no significance difference in the marginal stability boundary results obtained using the  $k-\epsilon$  and the SST Models. Because of the differences in the pressure drop predictions by the two different codes, there were significant differences between the results of the CFD and 1-D codes obtained.

Xie *et al.*<sup>[27]</sup> performed a numerical study investigating flow instability and estimating temperature in a supercritical boiler. A time-domain approach was adopted to solve the governing equations after which numerical code in Fortran language was written for the resulting numerical equations. The numerical solution model was validated with experimental data in literature. The results show that the coolant flow is more stable in the parallel channels than in the single channel. Out of phase flow instability of the mass flow rate was obtained at the inlet of the parallel channels. Liu *et al.*<sup>[28]</sup> performed experimental and theoretical study investigating flow instability of supercritical CO<sub>2</sub> natural circulation loop. Effects of system pressure, inlet temperature, coefficient of local resistance on flow instability of CO<sub>2</sub> were investigated. It was observed that the relationship between the coolant inlet temperature and the threshold power for occurrence of flow instability is not linear. The stability of the supercritical CO<sub>2</sub> natural circulation loop system is favored by increasing the system pressure and local resistance coefficient in the cold section. The system stability is also favored by decreasing local resistance coefficient in the hot section. Yang and Shan<sup>[29]</sup> carried out experimental study to investigate flow instability of hydrocarbon fuel cyclohexane in horizontal tubes at supercritical pressures. The effects of the length and diameter of the tubes on the hydrodynamic characteristics of supercritical cyclohexane were investigated. A new correlation for supercritical fluids was developed to predict onset of flow instability at supercritical pressures based on the obtained experimental data and design and operational parameters. The hydrodynamic stability of the fluid is favored by decreasing the length of the tube whereas increasing the diameter of the tube favors hydrodynamic stability of the fluid. Liu *et al.*<sup>[30]</sup> performed numerical study investigating density wave oscillation DWO in a parallel multi-channel system with water at supercritical pressure. A time-domain model was adopted to obtain numerical simulation results in this study. The numerical model was validated with existing experimental data in literature. Out-of-phase oscillation was observed in the parallel

channels that were perturbed and the system oscillation period and stability were not influenced by the number of perturbation channels. System stability is favored by the pressure increase. The worst stability of the system was observed at the critical inlet temperature below which the stability of the system decreases and above which the stability of the system increases. The occurrence of the DWO is attributed to the variation in the fluid density as the fluid inlet temperature is increased. Liu *et al.*<sup>[31]</sup> used the same time-domain model investigating the effects of wall thickness and pipe length on DWO by developing equations accounting for the storage of heat in a metal wall and a convective heat transfer. The storage of heat in the wall has influence on flow instability. For the situation where the thickness of the wall is zero (no storage of heat in the wall), the stability of the system decreases with the increase of the pipe length. For the situation where there is storage of heat in the wall (the thickness of the wall is not zero), there is a critical pipe length below which the system stability decreases and above which the system stability increases.

Zhang *et al.*<sup>[32]</sup> performed numerical study investigating the influence of tube wall and fluid property variations on fluid flow, heat transfer and flow instability in a vertical tube with water at supercritical pressure. The results obtained show that at steady state conditions, heat transfer is not influenced by the wall thickness whereas at transient state heat transfer and flow oscillations are influenced by the wall thickness. Sharp variations in thermo-physical properties of the coolant, buoyancy and flow acceleration effects are reduced by the presence of wall thickness and hence suppressing the flow oscillations in the system. Wang *et al.*<sup>[33]</sup> carried out an experimental investigation studying flow instability characteristics in Circulating Fluidized Bed (CFB) boiler with ultra-supercritical water in water wall tubes. Three different regions of flow instability including Region 1-3 were identified with the increase of heat flux in this study. Region 1 and 2 oscillations are associated with low heat flux (or low Ntpc) whereas Region 3 is associated with large heat flux (or large Ntpc). Long periods and large amplitudes are also associated with Region 1 and 2 oscillations whereas Region 3 has short periods and small amplitudes of flow oscillations. Region 1 and 2 oscillations are system oscillations whereas Region 3 oscillations are DWOs. The study results also show that the studied system becomes more stable with increasing system pressure, inlet mass flow rate and inlet pressure drop coefficient. The studied system becomes less stable with increasing coolant inlet temperature. Der Lee and Chen<sup>[34]</sup> performed flow instability study by developing a nonlinear dynamic model. The model was applied to a uniform channel with water at supercritical pressures. Constant heat flux was applied to the channel. Flow

stability boundaries presented using stability maps, flow instability characteristics and parametric effects were investigated. The parametric studies on system stability suggest that increasing inlet flow resistance or enlarging the channel diameter would stabilize the system while increasing outlet flow resistance or lengthening the channel length would destabilize the system. These findings on geometric characteristics were also obtained by Yang and Shang<sup>[29]</sup>. It was also found that complex nonlinear phenomena (supercritical Hopf bifurcations and period-doubled bifurcations) could occur at the uniform channel with supercritical water and chaotic oscillations could also occur in the most unstable region of the system. Chen *et al.*<sup>[35]</sup> carried out flow instability study by developing one-dimensional transient model. The study was carried out at supercritical pressures in single and parallel channel geometries with water. The one-dimensional model code was validated using IAEA benchmark data and experimental data developed by Nuclear Power Institute of China. The one dimensional transient model was able to capture flow excursion instabilities and density wave oscillations at supercritical pressures. For the single-channel geometry, there is an increased in mass flow rate and stabilization of the system with increasing pressure drop across the channel. For both the single and parallel channel geometries, the stabilization of the system is favored by increasing inlet pressure drop, decreasing exit pressure drop and throttle effects. This study also shows that systems with vertical upward flows are more stable whereas systems with vertical downward flows are worst stable.

The results of the experimental study carried out by Xi show that the type of axial power distribution adopted in supplying heat to fluid flowing through heat transfer systems has significant effect on heat transfer and flow instability at supercritical pressures<sup>[3]</sup>. Similar observations were also made by Shitsi<sup>[1, 2]</sup>. The two flow instability analysis methods used to obtain flow instability boundaries were examined in this research using axially decreased and homogeneous Axial Power Shapes (ADPS and HAPS). The flow instability boundaries were developed adopting dimensional and Ambrosini's dimensionless parameters (dimensional and dimensionless stability diagrams). Data used in this research as well as the methodology have been published in previous numerical studies carried out by Shitsi *et al.*<sup>[1, 2, 5, 7]</sup> in addressing heat transfer and flow instability related issues at supercritical pressures. The contribution of this research is to find out the effects of the two general flow instability analysis methods on flow instability data described in terms of flow instability boundaries.

## MATERIALS AND METHODS

**Theory:** The reference experimental setup by Xi *et al.*<sup>[3]</sup> 3D Geometry and Physical models adopted in this research have been described into detail in the publications by Shitsi *et al.*<sup>[1, 2, 25]</sup>.

**Stability criteria:** Generally, the three similar dimensionless parameters based on 1D Model used to describe flow instability boundary are provided by Gomez *et al.*<sup>[8]</sup> and Ambrosini and Sharabi<sup>[9]</sup>. The one by Ambrosini is represented as (Eq. 1 and 2):

$$\text{Trans-pseudo-critical number : } N_{\text{TPC}} = \frac{\beta_{\text{PC}} Q_t}{C_{\text{p,PC}} M_t} \quad (1)$$

$$\text{Subcooling pseudo-critical number : } N_{\text{SPC}} = \frac{\beta_{\text{PC}}}{C_{\text{p,PC}}} (h_{\text{PC}} - h_{\text{in}}) \quad (2)$$

The one by Gomez is represented as (Eq. 3 and 4):

$$\text{Phase change number : } N_{\text{PCH}} = \frac{v_{\text{fgq}} P_H L_H}{h_{\text{fg}} A_{\text{x-s}} v_t G} \quad (3)$$

$$\text{Subcooling number : } N_{\text{SUB}} = \frac{(v_{\text{in}} - v_{\text{in}})(h_{\text{in}} - h_{\text{in}})}{v_{\text{in}} h_{\text{in}} - h_{\text{in}}} \quad (4)$$

And the one by Zhao is represented as (Eq. 5 and 6):

$$\text{Expansion number : } N_{\text{EXP}} = \frac{R q P_h L}{P_{\text{Cp}} A_c u_{\text{in}}} \quad (5)$$

$$\text{Pseudo subcooling number : } N_{\text{PSUB}} = \frac{(h_A - h_{\text{in}})(\rho_A - \rho_B)}{h_{\text{AB}} \rho_B} \quad (6)$$

where, the terms  $\beta_{\text{pc}}$ ,  $C_{\text{p,pc}}$  and  $h_{\text{pc}}$  are respectively volume expansivity, specific heat and enthalpy at pseudo-critical point and  $Q_t$ ,  $M_t$  and  $h_{\text{in}}$  are respectively total heating power, total mass flow rate and inlet enthalpy of the coolant. The other undefined terms have their usual meanings.

These 1D dimensionless parameters cannot be adopted to describe flow instability boundary in 3D analysis because of assumptions made in their derivations including the frictional pressure drop coefficient is thought to be constant which is different from reality<sup>[3, 22]</sup>. According to Xi<sup>[3, 22]</sup>, the coolant inlet temperature and the ratio of heating power (threshold or critical power) to inlet mass flow rate are adopted to obtain the instability boundary for 3D analysis. But some studies also adopted the parameters, heating power or heating

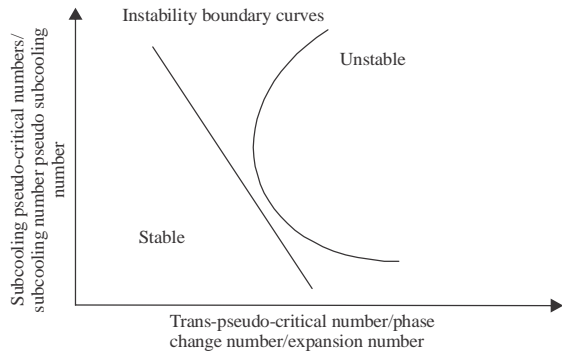


Fig. 1: Dimensionless stability diagram for describing flow instability of a system

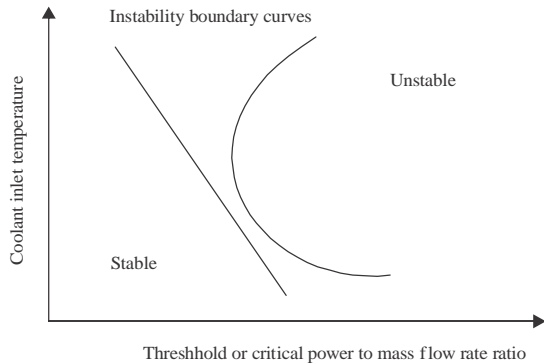


Fig. 2: Dimensional stability diagram for describing flow instability of a system

parameters, heating power or heating flux against inlet enthalpy or inlet temperature to obtain the instability boundary for 3-D analysis<sup>[18, 23, 24]</sup>. Figure 1 and 2, respectively show dimensionless and dimensional stability diagrams for describing flow instability of a system. Operating conditions to the left of the instability boundary curves are referred to as “Stable region” to operate a system. Similarly, the operating conditions to the right of the instability boundary curves are referred to as “Unstable region” to operate a system. The trends of flow instability results obtained and described in stability diagrams are almost linear or curves in most cases.

## RESULTS AND DISCUSSION

**Time step, grid and turbulence model considerations:** In this research, the coolant inlet temperature and the ratio of heating power (threshold or critical power) to inlet mass flow rate and Ambrosini’s dimensionless parameters ( $N_{TPC}$  and  $N_{SPC}$ ) were adopted to obtain the instability boundary for 3D analysis, methods already adopted by Xi<sup>[3, 22]</sup>, Ambrosini and

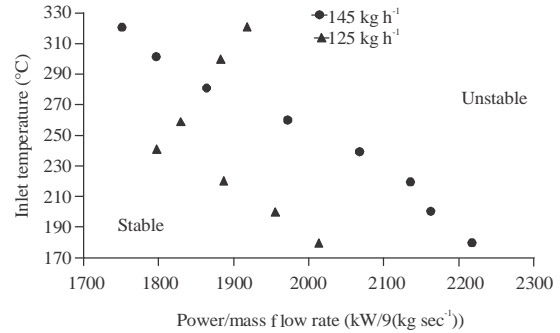


Fig. 3: Effect of mass flow rate adopting ADPS ( $p = 23$  MPa with gravity)

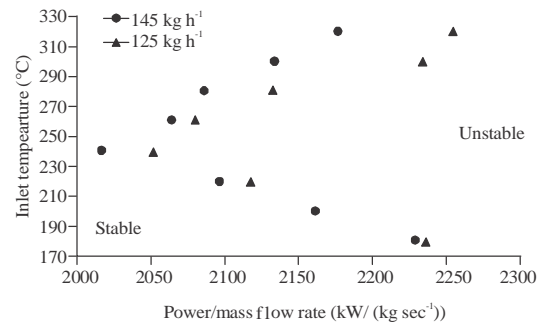


Fig. 4: Effect of mass flow rate adopting HAPS ( $p = 23$  MPa with gravity)

Sharabi<sup>[9]</sup>, Xiong *et al.*<sup>[20]</sup> and Zhang *et al.*<sup>[21]</sup>. Time step of 0.01 sec, Standard k-Epsilon turbulence model and mesh size of 2 785 000 cells established by Shitsi<sup>[1, 2, 25]</sup> were adopted in carrying out this study.

**Effect of mass flow rate on flow instability:** Axially decreased and homogeneous axial power shapes were considered in this research. For axially Decreased power shape ADPS, the heat flux applied to the inlet of the heated section was more than the heat flux applied to the outlet of the heated section and for homogeneous axial power shape HAPS constant heat flux was applied to the heated section. Two mass flow rates 125 kg h<sup>-1</sup> and 145 kg h<sup>-1</sup> were used for the numerical simulations. For ADPS, 20.75 kW was applied to each heated inlet section for 125 kg h<sup>-1</sup> and 24.0 kW was applied to each heated inlet section for 145 kg h<sup>-1</sup><sup>[22]</sup>. The heated section was divided into inlet and outlet heated sections for ADPS.

Figure 3 and 4 show the influences of mass flow rate on flow instability adopting ADPS and HAPS, respectively for inlet temperatures varying from 180, 320°C, system pressure of 23 MPa, total mass flow rates of 125 and 145 kg h<sup>-1</sup> and with the influence of gravity. For a system with ADPS or HAPS and operated

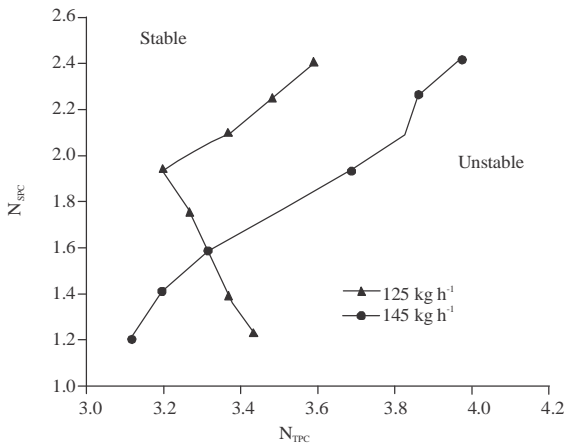


Fig. 5: Effect of mass flow rate adopting ADPS ( $p = 23$  MPa with gravity)

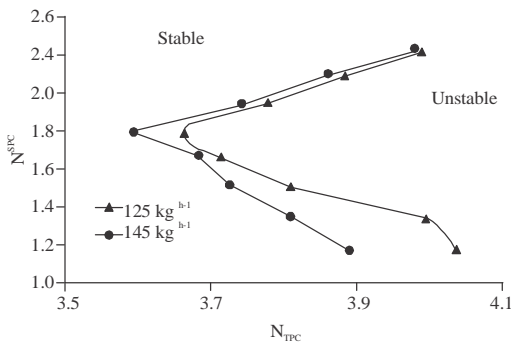


Fig. 6: Effect of mass flow rate adopting HAPS ( $p = 23$  MPa with gravity)

with  $125 \text{ kg h}^{-1}$  mass flow rate, there is a threshold power with particular inlet temperature below which stability decreases and above which stability increases with inlet temperature (there are both lower threshold for which stability decreases and upper threshold for which stability increases with increasing temperature). For a system operated with  $145 \text{ kg h}^{-1}$ , the observed stability behavior for the system with HAPS is similar to that of the system with HAPS or ADPS and operated at  $125 \text{ kg h}^{-1}$  but there is only lower threshold for the system with ADPS and the stability decreases with inlet temperature. With the increase of the system mass flow rate, the system with ADPS becomes more stable at low inlet temperatures and less stable at high inlet temperatures whereas the system with HAPS becomes less stable for the various inlet temperatures. For most of the inlet temperatures, the system with HAPS is more stable than that with ADPS for both mass flow rates. These results are also presented, respectively adopting dimensionless parameters (Fig. 5 and 6). It can be observed that the stability of the system decreases with increasing coolant inlet temperature up to a certain limiting threshold point and increases thereafter for dimensional stability figures

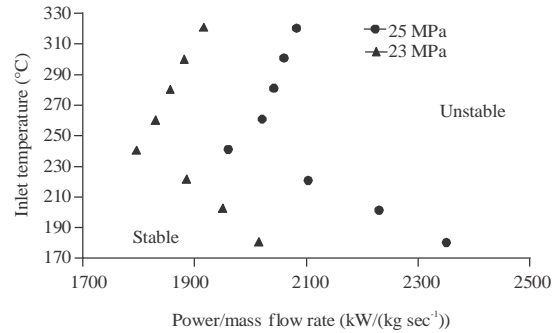


Fig. 7: Effect of system pressure adopting ADPS ( $M_t = 125 \text{ kg h}^{-1}$  with gravity)

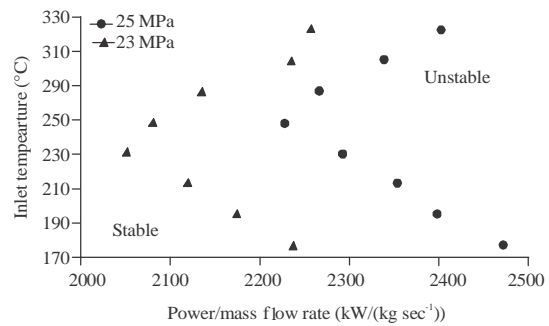


Fig. 8: Effect of system pressure adopting HAPS ( $M_t = 125 \text{ kg h}^{-1}$  with gravity)

(Fig. 5 and 6). For the case of the dimensionless stability figures (Fig. 7 and 8), stability of the system decreases with decreasing subcooling pseudo-critical number  $N_{SPC}$  (i.e., increasing coolant inlet temperature) up to a certain limiting threshold point and increases thereafter. The reversal in the observed trends is due to the trend of values produced by the expression  $(h_{pc} - h_{in})$  in the  $N_{SPC}$  relation (Eq. 15). The trend of values produced by the expression  $(h_{pc} - h_{in})$  decreases with increasing coolant inlet temperature (increasing coolant enthalpy). The pseudo-critical enthalpy  $h_{pc}$  is constant and has a value of  $2124.1 \text{ kJ kg}^{-1}$  at  $23 \text{ MPa}$  and  $377.5^\circ\text{C}$  and a value of  $2160.6 \text{ kJ kg}^{-1}$  at  $25 \text{ MPa}$  and  $384.9^\circ\text{C}$ . It can also be observed that the observations made for mass flow rate effects on flow instability using dimensional stability figures (Fig. 3 and 4) could also be made using dimensionless stability figures (Fig. 5 and 6).

**Effect of system pressure on flow instability:** Figure 7 and 8 show influences of system pressure on flow instability at system mass flow rate of  $125 \text{ kg h}^{-1}$  and with gravity adopting ADPS and HAPS, respectively. At both system pressures of  $23$  and  $25 \text{ MPa}$ , there is different threshold power for each pressure below which stability decreases and above which stability increases with inlet

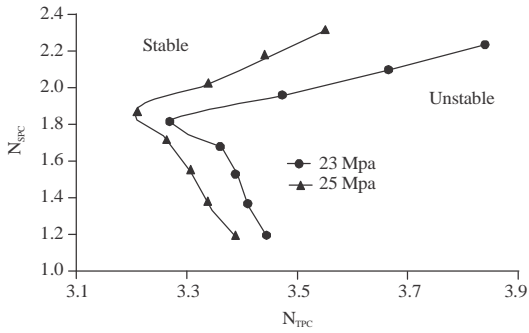


Fig. 9: Effect of system pressure adopting ADPS ( $M_t = 125 \text{ kg h}^{-1}$  with gravity)

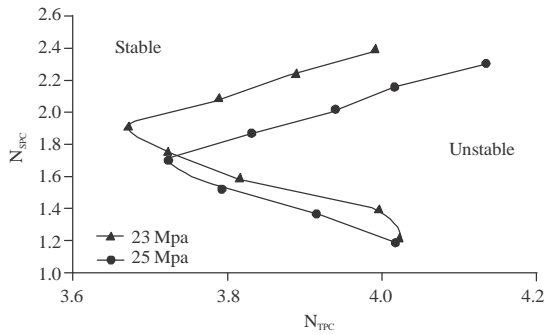


Fig. 10: Effect of system pressure adopting HAPS ( $M_t = 125 \text{ kg h}^{-1}$  with gravity)

temperature for a system with ADPS or HAPS. The system operated at high pressure is more stable than that operated at low pressure for a system with ADPS or HAPS. The system with HAPS is more stable than that with ADPS at both system pressures. These results are also presented adopting dimensionless parameters (Fig. 9 and 10). The observations made for influence of pressure on flow instability adopting ADPS and dimensional stability diagram (Fig. 7) could also be made for influence of pressure on flow instability adopting ADPS and dimensionless stability diagram (Fig. 9). The system operated under HAPS is more stable at high pressures adopting dimensional stability diagram (Fig. 8). The system operated under HAPS is more stable when  $N_{SPC}$  is high and less stable when  $N_{SPC}$  is low at high pressures adopting dimensionless stability diagram (Fig. 10). Similar observations were made by Su *et al.*<sup>[24]</sup> 2013, Xi *et al.*<sup>[32]</sup> and Xiong *et al.*<sup>[30]</sup>. It can also be observed that the observation, the system with HAPS is more stable than that with ADPS at both system pressures, obtained adopting dimensional stability diagrams (Fig. 7 and 8) could be obtained adopting dimensionless stability diagrams (Fig. 9 and 10).

**Effect of gravity on flow instability:** Figure 11 and 12 show influences of gravity on flow instability at system

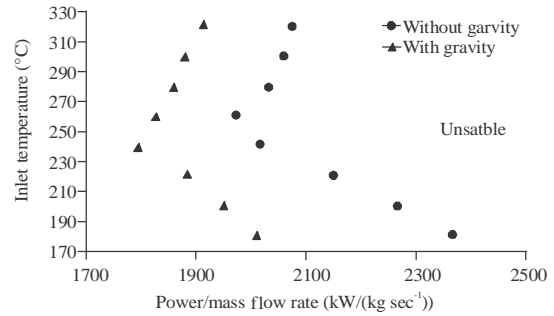


Fig. 11: Effect of gravity adopting ADPS ( $p = 23 \text{ MPa}$ ,  $M_t = 125 \text{ kg h}^{-1}$ )

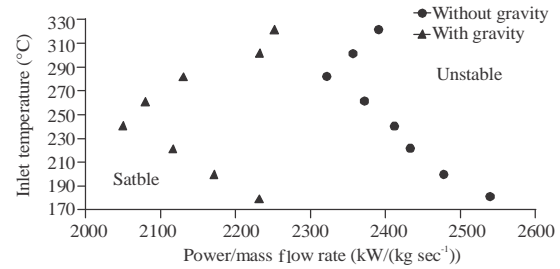


Fig. 12: Effect of gravity adopting HAPS ( $p = 23 \text{ MPa}$ ,  $M_t = 125 \text{ kg h}^{-1}$ )

mass flow rate of  $125 \text{ kg h}^{-1}$ , pressure of  $23 \text{ MPa}$  and with gravity or without gravity adopting ADPS and HAPS, respectively. For the system with ADPS or HAPS and operated with gravity or without gravity influence, there is a different threshold power for each system below which stability decreases and above which stability increases with inlet temperature. The system operated without gravity influence is more stable than that operated with gravity influence for the system with ADPS or HAPS. Similar, finding was obtained by Xi *et al.*<sup>[22]</sup>. The system with HAPS is more stable than that with ADPS. These results are also presented adopting dimensionless parameters (Fig. 13 and 14). The observations made for effects of gravity on flow instability adopting dimensional stability diagrams (Fig. 11 and 12) could also be made adopting dimensionless stability diagrams (Fig. 13 and 14).

**Comparison of numerical results with experimental results:** Figure 15 shows numerical and experimental instability boundaries for axially decreased and homogeneous axial power shapes at system mass flow rate of  $125 \text{ kg h}^{-1}$ , pressure of  $23 \text{ MPa}$ , inlet temperatures from  $180\text{-}260^\circ\text{C}$  and with gravity. For ADPS, the system stability decreases with decreasing subcooling pseudo-critical number  $N_{SPC}$  (i.e., increasing inlet temperature) up to the threshold points of  $(3.47, 2.00)$  for numerical



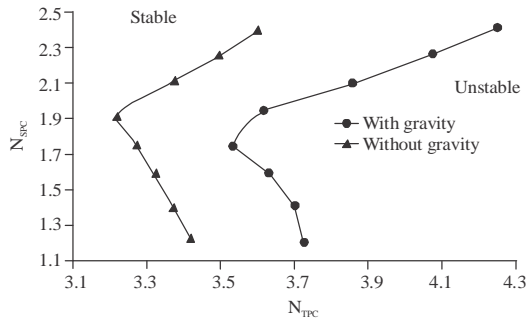


Fig. 13: Effect of gravity adopting ADPS ( $p = 23 \text{ MPa}$ ,  $M_i = 125 \text{ kg h}^{-1}$ )

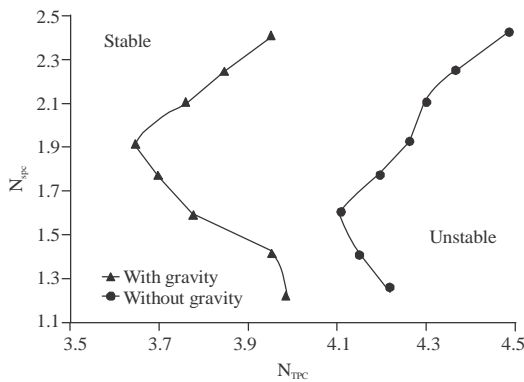


Fig. 14: Effect of gravity adopting HAPS ( $p = 23 \text{ MPa}$ ,  $M_i = 125 \text{ kg h}^{-1}$ )

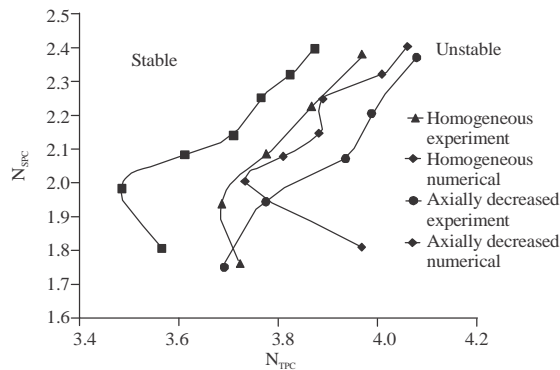


Fig. 15: Comparison between numerical and experimental results, Instability boundaries (Axially decreased and Homogeneous axial power distributions)

simulation and (3.73, 2.00) for experiment. The stability then increases with decreasing  $N_{SPC}$  after the threshold points. The threshold points (3.47, 2.00) and (3.73, 2.00) correspond to (67.5 kW, 232.5°C) and (72.5 kW, 232.5°C), respectively. For HAPS, the stability of the system decreases with decreasing  $N_{SPC}$  up to the threshold point of (3.68, 1.95) for numerical simulation. The

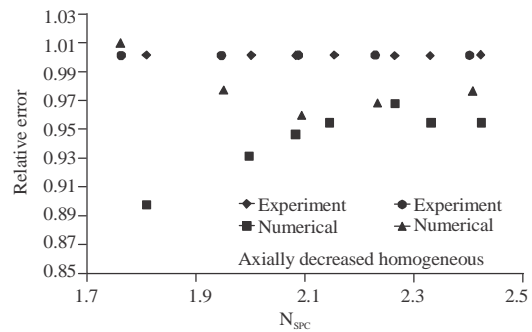


Fig. 16: Comparison between numerical and experimental results (Axially decreased and homogeneous axial power distributions)

stability of the system increases with decreasing  $N_{SPC}$  after the threshold point. There is only upper threshold for HAPS experimental trend and stability of the system decreases with decreasing  $N_{SPC}$ . The threshold point of (3.68, 1.95) corresponds to (71.4 kW, 238.7°C). Both the numerical and experimental homogeneous axial power shapes are more stable than the corresponding numerical and experimental axially decreased power shapes. Figure 16 and Table 1 quantitatively compare the numerical and experimental results of ADPS and HAPS at operating conditions of 23 MPa, 125 kg h<sup>-1</sup> and with gravity and most of the numerical results are within the acceptable error limit of  $\pm 10\%$ . But the 3D numerical tool adopted mostly under-predicted the experimental results for both axial power shapes. The numerical tool predicted experimental results quite better for the system with HAPS than that with ADPS.

Figure 17 and 18 show numerical and experimental inlet mass flow oscillations at 23 MPa, 125 kg h<sup>-1</sup>, 192°C and with gravity for ADPS with a heating power of 81.5 kW. For the total heating power of 81.5, 20.75 kW was applied to the heating wall of each inlet heated section for 78 sec and 4.71, 6.66 and 8.62 kW were applied to the heating wall of each outlet heated section for 26 sec, respectively. These system parameter values for axially decreased power shape are summarized in Table 2. Maximum amplitudes of 7.2 and 25 kg h<sup>-1</sup> were obtained for numerical and experimental results and periods of 1.0 and 1.3 sec were obtained for numerical and experimental results, respectively. The numerical tool adopted largely under-predicted experimental amplitude and quite well predicted experimental period of the inlet mass flow oscillations. The differences in the numerical amplitude and period of the oscillations compared to that of the experiments might be due to the use of larger time step because of computational time cost and also the inability of the turbulence model adopted to accurately capture the experimental amplitude and period of the oscillations.



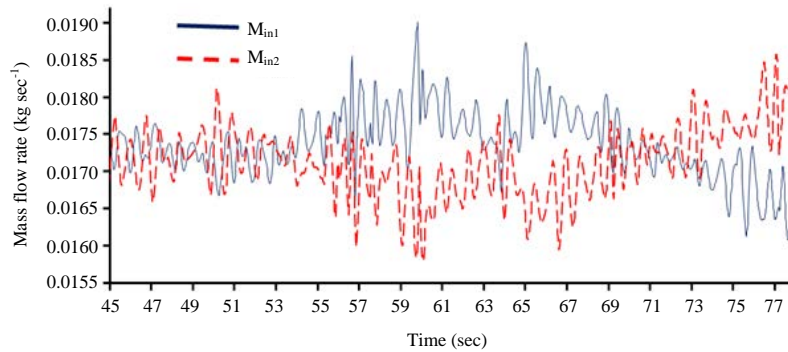


Fig. 17: Inlet mass flow rate oscillation of each channel (Numerical)<sup>[2]</sup>

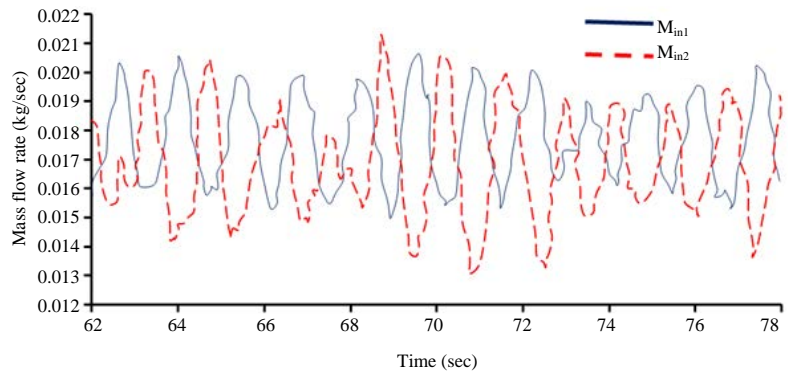


Fig. 18: Inlet mass flow rate oscillation of each channel (Experiment)<sup>[2]</sup>

Table 1: Numerical threshold power compared with experimental threshold power<sup>[2]</sup>

Homogeneous axial power distribution			Axially decreased power distribution		
Inlet temperature (°C)	Experimental threshold power (kW)	Numerical threshold power (kW)	Inlet temperature (°C)	Experimental threshold power (kW)	Numerical threshold power (kW)
182.5	79.2	77.3	180.0	78.8	75.2
203.8	77.5	75.1	191.3	77.8	74.3
221.3	76.4	73.3	200.1	75.5	73.0
238.7	73.1	71.4	214.0	75.4	71.9
260.0	71.6	72.2	222.4	73.9	69.9
	232.5	72.5	67.5		
	254.8	77.1	69.2		

Table 2: System parameter values for axially decreased power shape<sup>[2]</sup>

Parameters	Heating power and time of heat application				
	Each inlet heated section		Each Outlet heated section		
	Values	Power (kW)	Time (sec)	Power (kW)	Time (sec)
Inlet temperature (°C)	190	20.75	78.0	4.71	26.0
Pressure (MPa)	23			6.66	26.0
Mass flow rate (kg h <sup>-1</sup> )	125			8.62	26.0

**Flow instability studies conducted in parallel channel system geometry adopting Ambrosini’s dimensionless parameters for the results analysis:** Table 3 presents flow instability studies carried out using Ambrosini’s dimensionless parameters.

**Flow instability studies conducted in parallel channel system geometry adopting dimensional parameters for the results analysis:** Table 3 presents flow instability

studies carried out using dimensional parameters. The studies carried out by various researchers and presented in sections 4.5 and 4.6 show that flow instability analysis results obtained at supercritical pressures in parallel channels were mostly presented using dimensional flow instability analysis method. Similar findings were obtained by the two flow instability analysis methods which is in agreement with the findings obtained in this research.

Table 3: Flow instability analysis carried out using Ambrosini's dimensionless parameters

Authors	Heat distribution type	Key findings
Su <i>et al.</i> <sup>[24]</sup>	Homogeneous/constant axial power distribution	The system stability increases with increasing pressure, increasing mass flow rate and increasing frictional pressure drop
Xiong <i>et al.</i> <sup>[20]</sup> Liu <i>et al.</i> <sup>[36]</sup>	Homogeneous/constant axial power distribution Homogeneous/constant axial power distribution	System flow stability is favored by increase in pressure There is good agreement between the marginal stability boundaries obtained by using frequency-domain and time-domain methods
Zhang <i>et al.</i> <sup>[21]</sup>	Homogeneous/constant axial power distribution	Flow instability does not occur when the fluid temperature at the exit of the heated channels is below the pseudo-critical temperature irrespective of the amount of heating power, inlet temperature, system pressure and local loss coefficient adopted in the experiment
Wang <i>et al.</i> <sup>[33]</sup>	Homogeneous/constant axial power distribution	Region 1, 2 and density wave Oscillations were observed. Region1 and Region2 oscillations occurred when the heat flux is low whereas DWOs occur when the heat flux is relatively higher
Der Lee <i>et al.</i> <sup>[37]</sup>	Homogeneous/constant axial power distribution	Increasing inlet flow resistance or enlarging the channel diameter could stabilize the system while increasing outlet flow resistance or lengthening the channel length would destabilize the system
Wang <i>et al.</i> <sup>[28]</sup>	Homogeneous/constant axial power distribution	Decrease in tube length, increase in tube diameter, increase in inlet pressure drop coefficient and decrease in outlet pressure drop coefficient favors the stability of the parallel channel system

Table 4: Flow instability analysis carried out using dimensional parameters

Authors	Heat distribution type	Key findings
Hou <i>et al.</i> <sup>[23]</sup>	Uniformly axial power distribution, cosine-shaped or fork/stair-shaped axial power distributions	Systems with uniformly axial power distribution are more unstable than those with cosine-shaped or fork/stair-shaped axial power distributions
Su <i>et al.</i> <sup>[24]</sup>	Homogeneous/constant axial power distribution	System stability increases with increasing pressure, increasing mass flow rate and increasing frictional pressure drop
Liu <i>et al.</i> <sup>[36]</sup>	Homogeneous/constant and cosine-like axial power distributions	Stability of the parallel channel system is favored by increasing the mass flow rate
Li <i>et al.</i> <sup>[19]</sup>	Homogeneous/constant axial power distribution	System stability increases with inlet mass flow rate and the effect of in-let temperature on flow instability is not linear
Xi <i>et al.</i> <sup>[22]</sup>	Homogeneous/constant axial power distribution	Flow instability is influenced by system pressure, mass flow rate and gravity
Shitsi <i>et al.</i> <sup>[11]</sup>	Constant, uniform, axially decreased and axially increased power distributions	Flow instability is influenced by the type of axial power distribution supplying heat to the heated channels of the parallel channel system. Only lower boundary or both lower and upper boundaries are obtained as flow instability boundaries
Xi <i>et al.</i> <sup>[3]</sup>	Homogeneous/constant and axially decreased power distribution	The system is more stable with homogeneous axial power shape. The system becomes unstable with the increase of mass flow rate at high power boundary
Xiong <i>et al.</i> <sup>[20]</sup>	Homogeneous/constant axial power distribution	Increase in pressure or decrease in coolant inlet temperature favors the stability of the coolant flow in the parallel channels
Zhang <i>et al.</i> <sup>[21]</sup>	Homogeneous/constant axial power shape	Type I and Type II dynamic instabilities occur in the parallel channels. Type I in-stability occurs at low heating powers with long period of oscillation (20-300 sec) whereas type II instability occurs at high heating powers with short period of oscillation (2-5 sec)
Wang <i>et al.</i> <sup>[33]</sup>	Homogeneous/constant axial power distribution	Increase in inlet mass flow rate, pressure and inlet pressure drop coefficient favors system stability. Increase of inlet water temperature makes the system more unstable

### CONCLUSION

This study compares results from two flow instability analysis methods used to obtain flow instability boundary

results using axially decreased and homogeneous axial power shapes/distributions. The flow instability boundaries were developed adopting both dimensional and Ambrosini's dimensionless parameters (dimensional

and dimensionless stability diagrams). This study also examines the influences of parameters including mass flow rate, pressure and gravity on flow instability at supercritical pressures in parallel channel system. The results of the study show that both the dimensional and dimensionless stability diagrams could be used for flow instability analysis as the two different types of stability diagrams almost produced the same findings in this research. The following additional findings were obtained during the investigation using both the dimensional and dimensionless stability diagrams:

At low or high system pressures and low mass flow rates for system operated with or without gravity influence, stability of the system with HAPS (homogeneous axial power shape) or ADPS (Axially Decreased Power Shape) decreases and increases, respectively below and above a certain threshold power with inlet temperature.

At high mass flow rates, there is a threshold power below which stability decreases and above which stability increases with inlet temperature for HAPS but there is only lower threshold for ADPS and the stability decreases with inlet temperature. The system with HAPS is more stable than that with ADPS.

The system with ADPS or HAPS becomes more stable with the change of the system operated with gravity influence to the system operated without gravity influence and also with the increase of system pressure. With the increase of the system mass flow rate, the system with ADPS becomes more stable at low inlet temperatures and less stable at high inlet temperatures whereas the system with HAPS becomes less stable for the various inlet temperatures. The type of axial power shape adopted in supplying heat to the fluid flowing through heat transfer system has significant effect on the stability of the system. The 3D numerical tool, STAR-CCM+CFD code could predict flow instability in the parallel channels irrespective of the type of axial power shape adopted.

The numerical tool could predict experimental results quite better for a system with HAPS than that with ADPS. The numerical tool adopted largely under-predicted experimental amplitude and quite well predicted experimental period of the inlet mass flow oscillations. Supercritical systems operated under 25 MPa are more stable than those operated under 23 MPa. Both the dimensional and dimensionless stability diagrams could be used for flow instability analysis as the two different types of stability diagrams almost produced the same findings in this research.

#### **ACKNOWLEDGEMENTS**

Cd-Adapco is acknowledged for providing a reduced fee academic license and technical support in making this work possible.

#### **REFERENCES**

01. Shitsi, E., S.K. Debrah, V.Y. Agbodemegbe and E. Ampomah-Amoako, 2017. Numerical investigation of flow instability in parallel channels with supercritical water. *Ann. Nucl. Energy*, 110: 196-207.
02. Shitsi, E., S.K. Debrah, V.Y. Agbodemegbe and E. Ampomah-Amoako, 2018. Effect of axial power distribution on flow instability in parallel channels with water at supercritical pressures. *Ann. Nucl. Energy*, 112: 109-119.
03. Xi, X., Z. Xiao, X. Yan, T. Xiong and Y. Huang, 2014. Numerical simulation of the flow instability between two heated parallel channels with supercritical water. *Ann. Nucl. Energy*, 64: 57-66.
04. Tong, L.S. and Y.S. Tang, 1997. *Boiling Heat Transfer and Two-Phase Flow*. 2nd Edn., Taylor & Francis Publisher, New York, USA.,.
05. Yu, L., A. Sur and D. Liu, 2015. Flow boiling heat transfer and two-phase flow instability of nanofluids in a minichannel. *J. Heat Transfer*, Vol. 137, 10.1115/1.4029647
06. Ampomah-Amoako, E., 2013. Stability and control of SCWR systems: A study into concepts and applications. Ph.D. Thesis, Graduate School, University of Ghana, Legon, Accra, Ghana.
07. Nayak, A.K. and P.K. Vijayan, 2008. Flow instabilities in boiling two-phase natural circulation systems: A review. *Sci. Technol. Nucl. Install.*, 1: 1-15.
08. Gomez, T.O., A. Class, R.T. Lahey Jr. and T. Schulenberg, 2008. Stability analysis of a uniformly heated channel with supercritical water. *Nucl. Eng. Des.*, 238: 1930-1939.
09. Ambrosini, W. and M. Sharabi, 2008. Dimensionless parameters in stability analysis of heated channels with fluids at supercritical pressures. *Nucl. Eng. Des.*, 238: 1917-1929.
10. Ambrosini, W. and M.B. Sharabi, 2007. Assessment of stability maps for heated channels with supercritical fluids versus the predictions of a system code. *Nucl. Eng. Technol.*, 39: 627-636.
11. Ambrosini, W., 2007. On the analogies in the dynamic behaviour of heated channels with boiling and supercritical fluids. *Nucl. Eng. Des.*, 237: 1164-1174.
12. Sharabi, M.B., 2008. CFD analyses of heat transfer and flow instability phenomena relevant to fuel bundles in supercritical water reactors. Ph.D. Thesis, University of Pisa, Pisa, Italy.
13. Gomez, T.O., 2009. Stability analysis of the high performance light water reactor. Ph.D. Thesis, Institute for Nuclear and Energy Technologies, University of Karlsruhe, Karlsruhe, Germany.

14. Ambrosini, W., 2011. Discussion of similarity principles for fluid-to-fluid scaling of heat transfer behaviour at supercritical pressures. *Nucl. Eng. Des.*, 241: 5149-5173.
15. Ampomah-Amoako, E. and W. Ambrosini, 2013. Developing a CFD methodology for the analysis of flow stability in heated channels with fluids at supercritical pressures. *Ann. Nuclear Energy*, 54: 251-262.
16. Debrah, S.K., W. Ambrosini and Y. Chen, 2013a. Discussion on the stability of natural circulation loops with supercritical pressure fluids. *Ann. Nuclear Energy*, 54: 47-57.
17. Debrah, S.K., W. Ambrosini and Y. Chen, 2013b. Assessment of a new model for the linear and nonlinear stability analysis of natural circulation loops with supercritical fluids. *Ann. Nucl. Energy*, 58: 272-285.
18. Xiong, T., X. Yan, S. Huang, J. Yu and Y. Huang, 2013. Modeling and analysis of supercritical flow instability in parallel channels. *Int. J. Heat Mass Transfer*, 57: 549-557.
19. Li, J., T. Zhou, M. Song, Q. Huo, Y. Huang and Z. Xiao, 2015. CFD analysis of supercritical water flow instability in parallel channels. *Int. J. Heat Mass Transfer*, 86: 923-929.
20. Xiong, T., X. Yan, Z. Xiao, Y. Li, Y. Huang and J. Yu, 2012. Experimental study on flow instability in parallel channels with supercritical water. *Ann. Nucl. Energy*, 48: 60-67.
21. Zhang, L., B. Cai, Y. Weng, H. Gu, H. Wang, H. Li and V. Chatoorgoon, 2016. Experimental investigations on flow characteristics of two parallel channels in a forced circulation loop with supercritical water. *Applied Therm. Eng.*, 106: 98-108.
22. Xi, X., Z. Xiao, X. Yan, Y. Li and Y. Huang, 2014. An experimental investigation of flow instability between two heated parallel channels with supercritical water. *Nucl. Eng. Des.*, 278: 171-181.
23. Hou, D., M. Lin, P. Liu and Y. Yang, 2011. Stability analysis of parallel-channel systems with forced flows under supercritical pressure. *Ann. Nucl. Energy*, 38: 2386-2396.
24. Su, Y., J. Feng, H. Zhao, W. Tian, G. Su and S. Qiu, 2013. Theoretical study on the flow instability of supercritical water in the parallel channels. *Progress Nucl. Energy*, 68: 169-176.
25. Shitsi, E., S.K. Debrah, V.Y. Agbodemegbe and E. Ampomah-Amoako, 2017. Numerical investigation of heat transfer in parallel channels with water at supercritical pressure. *Heliyon*, Vol. 3, No. 11. 10.1016/j.heliyon.2017.e00453.
26. Ebrahimnia, E., V. Chatoorgoon and S.J. Ormiston, 2016. Numerical stability analyses of upward flow of supercritical water in a vertical pipe. *Int. J. Heat Mass Transfer*, 97: 828-841.
27. Xie, B., D. Yang, W. Wang, X. Nie and W. Liu, 2017. Numerical analysis on the flow instability of parallel channels in water wall of an ultra-supercritical CFB boiler. *Int. J. Heat Mass Transfer*, 110: 545-554.
28. Liu, G., Y. Huang, J. Wang, F. Lv and S. Liu, 2017. Experimental research and theoretical analysis of flow instability in supercritical carbon dioxide natural circulation loop. *Applied Energy*, 205: 813-821.
29. Yang, Z. and Y. Shan, 2018. Experimental study on the onset of flow instability in small horizontal tubes at supercritical pressures. *Applied Therm. Eng.*, 135: 504-511.
30. Liu, J., H. Li, Q. Zhang, X. Kong and X. Lei, 2019. Numerical study on the density wave oscillation of supercritical water in parallel multichannel system. *Nucl. Eng. Des.*, 342: 10-19.
31. Liu, J., H. Li, X. Lei, K. Guo and L. Li, 2018. Numerical study on the effect of pipe wall heat storage on density wave instability of supercritical water. *Nucl. Eng. Des.*, 335: 106-115.
32. Zhang, Z., C. Zhao, X. Yang, P. Jiang, S. Jiang and J. Tu, 2019. Influences of tube wall on the heat transfer and flow instability of various supercritical pressure fluids in a vertical tube. *Applied Therm. Eng.*, 147: 242-250.
33. Wang, W., D. Yang, Z. Liang, M. Qu and S. Ouyang, 2019. Experimental investigation on flow instabilities of ultra-supercritical water in parallel channels. *Applied Thermal Eng.*, 147: 819-828.
34. Der Lee, J. and S.W. Chen, 2019. The dynamic analysis of a uniformly heated channel at a supercritical pressure using a simple nonlinear model. *Ann. Nucl. Energy*, 126: 95-109.
35. Chen, J., H. Gu and Z. Xiong, 2019. Development of one-dimensional transient model for predicting flow instability at supercritical pressures. *Progress Nucl. Energy*, 112: 162-170.
36. Liu, P., D. Hou, M. Lin, B. Kuang and Y. Yang, 2014. Stability analysis of parallel-channel systems under supercritical pressure with heat exchanging. *Ann. Nucl. Energy*, 69: 267-277.
37. Der Lee, J., S.W. Chen and C. Pan, 2019. Nonlinear dynamic analysis of parallel three uniformly heated channels with water at supercritical pressures. *Int. J. Heat Mass Transfer*, 129: 903-919.
38. Wang, W., D. Yang, L. Dong, J. Li, X. Zhou and W. Pan, 2020. Experimental and numerical study on density wave oscillations of supercritical water in parallel water wall channels of an ultra-supercritical circulating fluidized bed boiler. *Applied Therm. Eng.*, Vol. 165, 10.1016/j.applthermaleng.2019.114584.